Nonlinear Polarization Spectroscopy in the Frequency Domain of Light-Harvesting Complex II: Absorption Band Substructure and Exciton Dynamics

Heiko Lokstein,*‡ Dieter Leupold,‡ Bernd Voigt,‡ Frank Nowak,‡ Jürgen Ehlert,‡ Paul Hoffmann,* and Gyözö Garab§

*Institut für Biologie (Pflanzenphysiologie), Humboldt-Universität zu Berlin, D-10099 Berlin, Germany; ‡Max-Born-Institut für Nichtlineare Optik und Kurzzeitspektroskopie, D-12474 Berlin, Germany; and §Institute of Plant Biology, Hungarian Academy of Sciences, Szeged, Hungary

ABSTRACT Spectral substructure and ultrafast excitation dynamics have been investigated in the chlorophyll (Chl) *a* and *b* Q_y region of isolated plant light-harvesting complex II (LHC II). We demonstrate the feasibility of Nonlinear Polarization Spectroscopy in the frequency domain, a novel photosynthesis research laser spectroscopic technique, to determine not only ultrafast population relaxation (T_1) and dephasing (T_2) times, but also to reveal the complex spectral substructure in the Q_y band as well as the mode(s) of absorption band broadening at room temperature (RT). The study gives further direct evidence for the existence of up to now hypothetical "Chl forms". Of particular interest is the differentiated participation of the Chl forms in energy transfer in trimeric and aggregated LHC II. Limits for T_2 are given in the range of a few ten fs. Inhomogeneous broadening does not exceed the homogeneous widths of the subbands at RT. The implications of the results for the energy transfer mechanisms in the antenna are discussed.

INTRODUCTION

In higher plants the peripheral antennae of both photosystems I and II consist of a number of chlorophyll (Chl) *a/b* protein complexes. Most abundant and extensively studied is the main light-harvesting complex (LHC II) harboring >50% of the total Chl (*a* + *b*) in thylakoid membranes. Different preparations have been termed "LHC II"; in the following the term will be used only for the bulk complex comprising the *Lhcb1* and *Lhcb2* gene products, according to the nomenclature of Jansson (1994).

Very recently the 3D structure of LHC II has been obtained with 3.4 Å resolution (Kühlbrandt et al., 1994). The basic building unit appears to be a (mixed) trimer of the two apoproteins, in crystals as well as in vivo, with at least 12 Chls (*a* + *b*) non-covalently attached to each apoprotein (Kühlbrandt et al., 1994). However, at the current resolution Chls *a* and *b* were not discernible, so their assignment to specific binding sites remains tentative. The structure data indicate that the pigments are densely packed in the complex. The shortest center-to-center distances between the Chls range from 9 to 14 Å (Kühlbrandt et al., 1994). This renders strong excitonic interaction as well as ultrafast and efficient excitation energy transfer (EET) between neighboring Chls highly probable.

Besides its light-harvesting function, LHC II is assumed to play a key regulatory role in plant photosynthesis. The phosphorylation state of LHC II is thought to govern excitation distribution between photosystems I and II (state 1–state 2 transitions; cf., e.g., Allen, 1992). Furthermore, aggregation in vitro results in drastic changes in the fluorescence properties of LHC II: yield and lifetime(s) are lowered (Ide et al., 1987). Thus, it has been proposed that reversible aggregation of LHC II could establish the molecular basis of "high-energy quenching," an important physiological mechanism of safely dissipating excess excitation energy in photosystem II (Horton and Ruban, 1992; Mullineaux et al., 1993; Lokstein et al., 1993, 1994). However, the quenching species has not yet been identified.

Inasmuch as the intrinsic arrangement of the pigments governs the excited state dynamics in the complex, ultrafast spectroscopy may provide further insight into structure-function relationships. Much improved frequency and time domain techniques (with respect to spectral and temporal resolution) have revealed complex multiphasic excited state kinetics in LHC II with ultrafast components even in the 100-fs range (Eads et al., 1989; Kwa et al., 1992; Du et al., 1994; Palsson et al., 1994; Savikhin et al., 1994).

Such measurements and the interpretation of the data are, however, complicated by several factors: The $S_0 \rightarrow S_1$ (Q_y) absorption band of Chl *a* in LHC II (as in pigment-protein complexes in general) is considerably broadened and red shifted with respect to monomeric Chl *a* in organic solvents. This is generally interpreted in terms of spectral heteroge-

Received for publication 13 March 1995 and in final form 21 July 1995.

Address reprint requests to Dr. Heiko Lokstein, Institut für Biologie (Pflanzenphysiologie), Humboldt-Universität zu Berlin, Unter den Linden 6 (Sitz: Philippstr. 13), D-10099 Berlin, Germany. Tel.: 49-030-2895-677; Fax: 49-030-2895-537; E-mail: nowak@mbi.fta-berlin.de.

Abbreviations used in this article: CD, circular dichroism; Chl, chlorophyll; EET, excitation energy transfer; FWHM, full width at half maximum; Γ_{hom} and Γ_{inh}, homogeneous and inhomogeneous line-width, respectively; LHC II, light-harvesting Chl *a/b* complex associated with photosystem II; NLPF, nonlinear polarization spectroscopy in the frequency domain; psi type CD, polymerization or salt-induced type CD signals; RT, room temperature; S_0 and S_1, electronic ground state and first singlet-excited state, respectively; T_1 and T_2, energy and phase relaxation times, respectively.

0006-3495/95/10/1536/08 $2.00

neity, comprising several (strongly overlapping) "Chl forms" (e.g. Brown, 1972; French et al., 1972; Hemelrijk et al., 1992; Jennings et al., 1993). The molecular origin and physiological role of the "forms" is not yet established. Whether the forms comprise monomeric Chls in a different protein environment, excitonic components or a combination of both, has not been elucidated. Neither is the ratio of homogeneous to inhomogeneous broadening for the individual forms established.

A multitude of essentially indirect approaches to this issue (such as Gaussian analysis of the spectra and derivative spectroscopy) has been reported, yielding differing results (e.g., Brown, 1972; French et al., 1972; Brown and Schoch, 1981; Hemelrijk et al., 1992; Krawczyk et al., 1993; Jennings et al., 1993; Zucchelli et al., 1994). Recent ideas converge toward a consensus model in which at least six Chl forms are assumed to describe steady-state spectra of LHC II (Jennings et al., 1993). An earlier approach to the problem by means of nonlinear laser spectroscopy has been reported by Leupold et al. (1989). Induction of nonlinear absorption in the long-wavelength part of the Q_y-absorption band of chloroplast suspensions (by highly monochromatic sub-ns pulses at 687 and 692 nm) resulted in transient band-shape changes in the whole range of investigation (645–680 nm). This is in conflict with the model of Jennings et al. (1993), suggesting subbands characterized by band widths of 9–12 nm (full width at half maximum, FWHM), if these are not excitonic components.

To understand (and model) the abovementioned ultrafast EET times, a further problem has to be considered: excitation coherence, the decay of which is characterized by the phase or transversal relaxation time (T_2):

$$T_2^{-1} = (2T_1)^{-1} + (T_2^*)^{-1}; \quad (1)$$

where T_1 and T_2^* are energy relaxation time and pure dephasing time, respectively. T_2 is related to the homogeneous width (Γ_{hom}) by:

$$T_2 = \lambda^2/\pi c\Gamma_{hom}. \quad (2)$$

Characterization of dephasing by only one parameter is based on the assumption that the process is purely intramolecular. There are hints that for certain cyanine dyes in solution the opposite case may apply, indicating the need for a stochastic approach to describe the frequency fluctuations of the absorbing systems (Nibbering et al., 1991). Our data, however, suggest the validity of the assumption of intramolecular dephasing at least for cryptocyanine (D. Leupold, J. Ehlert, J. Hirsch, H. Stiel, K. Teuchner, and W. Sandner, unpublished results). Up to now, no relevant data for Chl systems are available.

The most common approach to describe EET assumes incoherent hopping between weakly coupled pigments as described by the Förster theory (Förster, 1948, 1965). Even for strongly coupled Chls (as has to be expected for LHC II) the incoherent approach may be justified if T_2 is much shorter than the transfer time (van Grondelle, 1985).

Theoretical estimates of the order of T_2 in photosynthetic antenna systems are controversial and experimental data for room temperature (RT) conditions are scarce. Kenkre and Knox (1976) have argued that T_2 is in the range of a few tens of fs. It should be noted that this is close to the recently inferred EET rates of 100 fs and less (Du et al., 1994). Thus, according to Eq. 1 EET may contribute effectively to phase destruction. However, Nedbal and Szöcs (1986) pointed out that a theory not restricted to the lowest orders of dipole-dipole interactions makes coherent motion of excitons for >1 ps probable. Indeed, Bittner et al. (1991) have derived T_2 values of ~1 ps from RT nonlinear absorption experiments in the Q_y region of a PS II preparation (BBY).

Another phenomenon observed upon aggregation of LHC II is the emergence of intensive nonconservative (so-called "psi type") bands in the circular dichroism (CD) spectrum. This is usually interpreted in terms of reorganization of LHC II into large chiral macrodomains with long-range interaction between chromophores (Garab et al., 1988; Garab, 1993; Barzda et al., 1994). Theory for psi type aggregates (Keller and Bustamante, 1986) predicts delocalization of excitation energy over large arrays of chromophores.

We are currently exploring the potential of nonlinear polarization spectroscopy in the frequency domain (NLPF) to investigate biological systems at different levels of structural complexity. NLPF was first applied to condensed matter by Song et al. (1978) to determine ultrafast T_1 in dissolved organic dyes. Subsequent theoretical investigations have shown that the NLPF lineshapes contain further information, e.g., on the mode of band broadening, on the spectral cross-relaxation time T_3 (Neef and Mory, 1991), on spectral substructure (Leupold et al., 1994), and on EET (D. Leupold and V. May, manuscript in preparation). The principle of NLPF spectroscopy is comprehensively described elsewhere (Song et al., 1978; Saikan and Sei, 1983; Leupold et al., 1994); thus it is only briefly accounted for in Fig. 1.

NLPF has unique advantages when compared with established techniques with similar information content. 1) In contrast to, e.g., nonphotochemical hole-burning spectroscopy, it allows the investigation of biological objects at physiological temperatures, thus reducing the possibility of structural alterations in the samples upon cooling. 2) The determination of relaxation times in the ps/fs range with laser pulses in the ns range provides the possibility of probing with nearly monochromatic radiation (when compared with fs time-domain techniques). Leupold et al. (1992, 1993, 1994) have previously applied the NLPF technique to investigate the spectral substructure and excited state dynamics in purple bacterial antennae, revealing T_2 values in the sub-ps range at RT. Here we report on the first NLPF experiments with trimeric and aggregated samples of spinach LHC II.

MATERIALS AND METHODS

LHC II was prepared from spinach as described by Krupa et al. (1987). The final LHC II pellets were characterized by a Chl *a*/*b* ratio of 1.13 ± 0.04

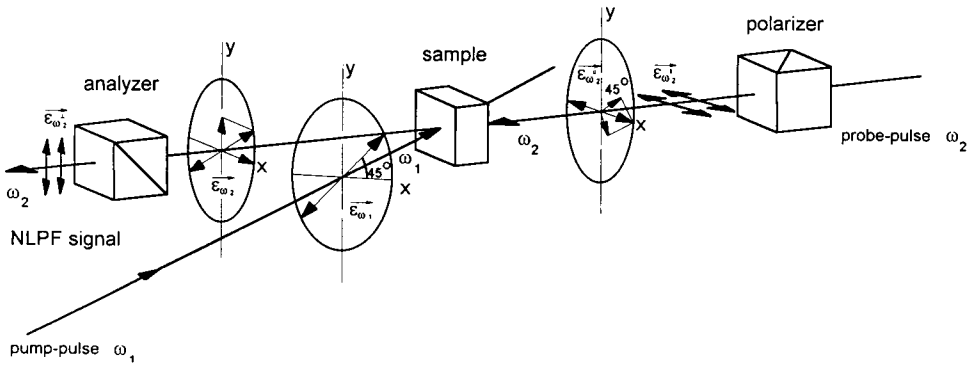

FIGURE 1 The principle of NLPF spectroscopy. The sample is probed by a highly monochromatic, linearly polarized beam (ω_2, fixed in the absorption band to be analyzed). The beam is blocked behind the sample by a perpendicularly oriented polarizer (analyzer). A pump beam (ω_1, variable in the same absorption band) and likewise linearly polarized (but at an angle of 45° with respect to the ω_2 polarization plane) induces dichroism and birefringence in the sample, thus generating a polarization component of the probe beam orthogonal to its original polarization. This component can be detected behind the analyzer, thus providing the NLPF signal, registered as a function of frequency difference between ω_1 and ω_2.

as determined in 80% acetone solution according to Arnon (1949). Fully denaturing SDS-PAGE analysis indicated the presence of essentially two apoproteins in the 25–27 kDa range (exceeding 95% of the total protein; data not shown but cf. also Krupa et al., 1987). For disintegration into trimers the LHC II pellet was solubilized with 0.5% *n*-octyl β-D-glucopyranoside + 0.5% digitonin (Mullineaux et al., 1993). Aggregation was induced by addition of 1 mM (final concentration) $MgCl_2$. The degree of aggregation was judged from CD and 77 K fluorescence emission spectra. CD spectra were recorded on a CD6 dichrograph (Jobin-Yvon, France). 77 K fluorescence emission spectra were recorded from samples containing 5 μg Chl/ml on a F-4500 fluorescence spectrophotometer (Hitachi) exciting at λ = 440 nm (slit widths of 5 and 2.5 nm, for excitation and emission, respectively). Absorption of the samples was adjusted and spectra were recorded using a Lambda 19 spectrophotometer (Perkin-Elmer Cetus, Norwalk, CT). NLPF experiments were performed with LHC II suspended in buffer (10 mM Tricine, pH 7.8) at 0.35 mg Chl/ml ($OD_{678} \approx 1.35$) in a 1-mm flow-through cell (to minimize sample degradation during the experiment). Absorption as well as RT and 77 K-fluorescence spectra recorded after the experiments gave no indication of sample degradation during the measurements (spectra not shown).

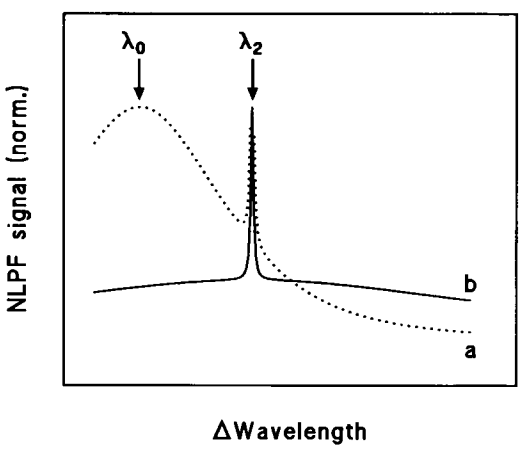

FIGURE 2 Theoretical NLPF lineshapes. *a*) A homogeneously broadened band (the bandshape of the individual species is identical with the shape of the global absorption band, with their respective maxima at λ_0). For $\lambda_2 \neq \lambda_0$ two maxima are observed in the NLPF signal, with one at $\lambda_1 = \lambda_2$ and a second at $\lambda_1 = \lambda_0$. For the special case that λ_2 is located at the half-width of the band both peaks will have the same height. *b*) An extremely inhomogeneous broadened band (the width of the distribution function of the individual transitions is much larger than the homogeneous width of each of them). Only a single symmetric signal centered around $\lambda_1 = \lambda_2$ is observed. Note that in this particular case there is no fingerprint of the overall absorption maximum. An intermediate case (not shown, here referred to as moderate inhomogeneous broadening) is characterized by a relatively large Γ_{hom} spread continuously over a certain distribution width.

The NLPF setup has been described previously (Leupold et al., 1992, 1993). Some modifications have been introduced since to enhance resolution, including 1) a selected pair of polarizers, 2) narrow-band dye lasers (spectral line-width: 0.05 cm^{-1}), and 3) a photomultiplier was used as detector. Pump and probe beams (pulse duration: 15 ns FWHM) were obtained from tunable LPD 3002 dye lasers (LAS, Stahnsdorf, Germany; laser dye: DCM/DMSO, tunable from 640 to 690 nm) synchronously pumped by an LPX 105 excimer laser (Lambda-Physik, Göttingen, Germany). The pump intensity was varied between 1.4×10^{24} and 4×10^{25} photons/$cm^2 \times$ s. The probe beam was three orders of magnitude less intense. NLPF is a technique for investigating processes preferably in the ps/fs-range; the actual time resolution limits depend on the experimental parameters (essentially on laser linewidth and tuning range). For the present setup the resolution range spans from ~10 fs up to 60 ps.

The NLPF signal function (S) can be analyzed for model systems solving the equations of motion for the density matrix of interest by third order perturbation theory (Song et al., 1978; Saikan and Sei, 1983; Neef and Mory, 1991). Already a simple two-level system (Fig. 2) or a model combining several such systems suffices to explain the principal features of NLPF spectra. From the theoretical lineshapes the following four principal cases can be distinguished (cf. also Leupold et al., 1994).

1) Pure homogeneous broadening:

$$S(\Delta;\, \omega_{02}) = |f_{hom}|^2 \tag{3}$$

$$= \alpha \frac{\gamma^2\Gamma^2\{4\Gamma^2 + 3\omega_{02}^2 + \omega_{01}^2\}^2 + \Delta^2\{2\Gamma(\Gamma^2 + \omega_{02}^2) + \gamma(\omega_{01}\omega_{02} - \Gamma^2)\}^2}{\gamma^2(\gamma^2 + \Delta^2)(\Gamma^2 + \omega_{01}^2)^2(\Gamma^2 + \omega_{02}^2)^2}$$

with f, lineshape function of the third order nonlinear polarization; $\gamma = T_1^{-1}$; $\Gamma = T_2^{-1}$; ω_1, frequency ($\omega = 2\pi c/\lambda$) of the pump beam (variable); ω_2, frequency of the probe beam (fixed); ω_{1_i}, frequency in the maximum of the distribution function of the transition frequency (in the homogeneous case termed ω_0); $\Delta = \omega_1 - \omega_2\omega_{ij} = \omega_i - \omega_j$; α = constant factor.

2) Extreme inhomogeneous broadening:

$$S(\Delta) = \alpha \frac{4\gamma^2 + \Delta^2}{(4\Gamma^2 + \Delta^2)(\gamma^2 + \Delta^2)} \tag{4}$$

3) Intermediate case, here referred to as moderate inhomogeneous broadening:

$$S(\Delta;\omega_{2L}) = \alpha\left|\frac{1}{\gamma}\frac{1}{\Gamma+\delta-i\omega_{1L}}+\frac{1}{\gamma+i\Delta}\frac{1}{\Gamma+\delta-i\omega_{2L}}+\left(\frac{1}{\gamma}+\frac{1}{g+i\Delta}\right)\frac{2(\Gamma+\delta)+i\Delta}{(\Gamma+\delta+i\omega_{1L})(2\Gamma+i\Delta)}\right|^2 \quad (5)$$

with δ, width of the distribution of the transition frequency.

Usually the situation will be even more complicated by overlap of several bands of one of the above types: 4) heterogeneous broadening (linear superposition of m, in this study, homogeneously broadened components with transition frequencies $\omega_{0;1}, \omega_{0;2}, \ldots, \omega_{0;m}$):

$$S(\Delta) = \left|\sum_{j=1}^{N} g_j f_j(\Delta, \omega_{0,j})\right|^2 \quad (6)$$

Parameters were extracted from the data by fitting the appropriate lineshape function to the experimental curve.

RESULTS AND DISCUSSION

Characteristic CD and 77 K fluorescence emission spectra of trimeric and aggregated LHC II are shown in Fig. 3. The spectra closely resemble those previously reported for LHC II in the respective states (cf. Ide et al., 1987; Bassi et al., 1991; Garab, 1993; Mullineaux, 1993). Whereas trimers give rise to a single 77 K emission band centered at ~682 nm, aggregates are characterized by the appearance of a second emission maximum at ~700 nm and a considerably lower fluorescence yield (note that the aggregate emission spectrum is magnified 15 times (Fig. 3 *insert*). In the CD spectrum typical psi type bands centered at 490 and 682 nm indicate formation of macroaggregates upon addition of Mg^{2+} (Garab et al., 1988; Garab, 1993).

The RT Q_y absorption spectrum of LHC II is considerably broadened with respect to monomeric Chl *a* in organic solvents. Besides the two maxima around 652 (Chl *b*) and 674 nm (Chl *a*) it appears to be rather featureless at RT in either the trimeric or the aggregated state, the latter being characterized by a slightly red-shifted Chl *a* maximum (to 676 nm, Fig. 4).

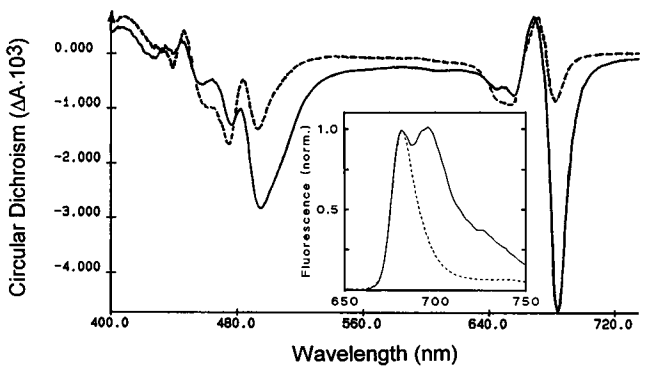

FIGURE 3 CD and normalized 77 K fluorescence emission spectra (*insert*) of trimeric (----) and aggregated LHC II (——).

NLPF spectra of LHC II

NLPF spectroscopy was performed (Fig. 4, *arrows*) at probe wavelengths (λ_2) of 645, 670, and 685 nm; for aggregates additionally at the respective absorption maximum of 676 nm. NLPF spectra were recorded in two regimes, 1) with high spectral resolution (1 pm steps) in the immediate vicinity of the resonance wavelength $\lambda_1 = \lambda_2$; and 2) with lower resolution (0.2 nm step width) over a large range of the Chl *a*/*b* Q_y band (across the entire tuning range of the pump beam λ_1) with otherwise identical instrument parameters. Whereas the high-resolution scan around the resonance wavelength contains mainly information on T_1 the broad-range scan carries information on the existence of spectral substructures as well as on their (or the overall) homogeneous and inhomogeneous widths and the corresponding T_2 (Neef and Mory, 1991; Leupold et al., 1994).

In Fig. 5 (*upper panel*) typical broad-range RT-NLPF spectra of trimeric LHC II, probed at 670 and 685 nm (Chl *a* region), are given. At first sight it is evident that for all spectra the case of extreme inhomogeneous broadening can be ruled out (cf. also Fig. 2 *b*), since, besides the resonance peak, a broad secondary maximum is obvious. Characteristic changes in the NLPF signal shape upon variation of λ_2 clearly indicate that there must be more than one distinguishable absorbing species, thus giving (according to our

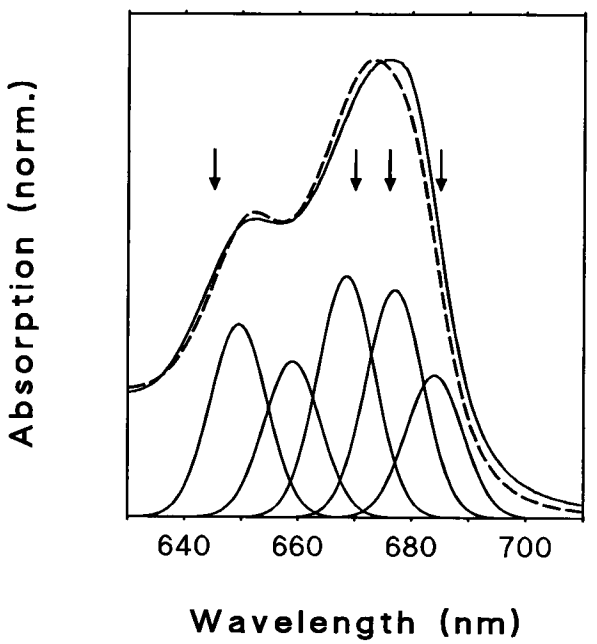

FIGURE 4 Q_y absorption spectra of trimeric (----) and aggregated (——) LHC II. Subbands according to Jennings et al. (1993) and NLPF probe wavelengths (645, 670, 676, and 685 nm; *arrows* from left to the right, respectively) are indicated.

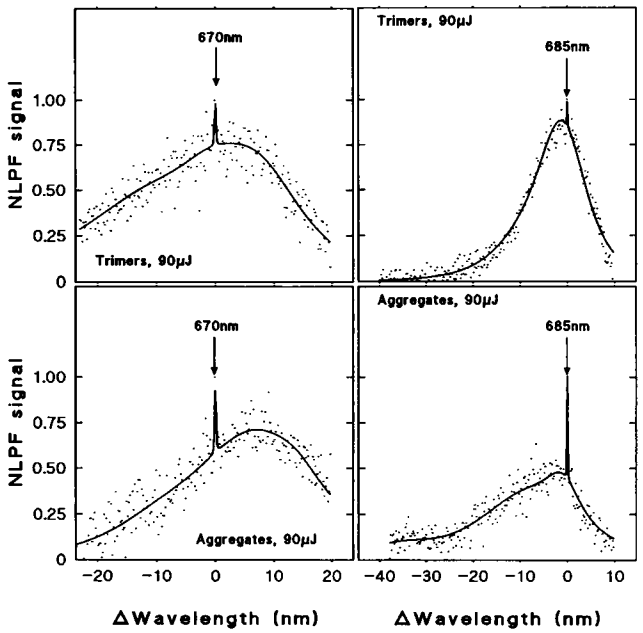

FIGURE 5 Experimental NLPF data and fits (——) assuming heterogeneity according to Jennings et al. (1993) and prevailing homogeneous broadening of the subbands in trimeric and aggregated LHC II. The samples were probed in the Chl *a* Q_y region at 670 and 685 nm. Note that the "spikes" at $\lambda_1 = \lambda_2$ are illustrative marks (e.g., when comparing with the theoretical picture of extreme inhomogeneous broadening). But they are not useful for direct quantitative evaluation; their actual FWHM is much smaller than the step width in the broad range measuring mode. The "spikes" are well resolved in the high-resolution scans, cf. Fig. 6.

knowledge) for the first time a direct hint toward the existence of distinct subbands (Chl forms).

Using the theoretical lineshape function for heterogeneous broadening and the center wavelengths of the subbands obtained by Jennings et al. (1993) we could fit our data (fits correspond to the solid lines in Fig. 5). The parameters extracted from the fits are displayed in Tables 1 and 2, and will be discussed in the following section.

In most cases, for probing at a certain λ_2 more than one subband gives a contribution to the overall NLPF signal. This can result either from direct contributions of subbands (Chl forms) with a broad Γ_{hom}, or may reflect indirect

TABLE 1 Coupling of Chl spectral forms in LHC II trimers and aggregates. λ_0 and λ_2 correspond to the center wavelengths of the individual subbands and the NLPF probe wavelengths, respectively

	Spectral forms in									
λ_2	LHC II trimers (λ_0 (nm))					LHC II aggregates (λ_0 (nm))				
(nm)	649	660	669	677	684	649	660	669	677	684
645	X	X	X	–	–	X	X	–*	X	–
670	–	X	X	X	–	–	–	–	X	–
676						X	–	–	X	X
685	–	–	–	X	X	X	–	–	X	X

*No 669-nm Chl form detectable in LHC II aggregates.

TABLE 2 Dephasing times (T_2) and corresponding homogeneous linewidths (Γ_{hom}) in trimeric and aggregated LHC II at room temperature

LHC II	649 nm	660 nm	669 nm	677 nm	684 nm
Trimers					
T_2 (fs)	10 ± 4	15 ± 5	21 ± 7	25 ± 8	40 ± 13
Γ_{hom} (cm^{-1})	1060	710	500	425	260
Aggregates					
T_2 (fs)	24 ± 8	24 ± 8	*	21 ± 7	60 ± 20
Γ_{hom} (cm^{-1})	440	440	*	500	175

The lower limits of T_2 represent the values obtained assuming pure homogeneous broadening, whereas the upper limits were derived for moderate inhomogeneous broadening of the respective subband.
*No 669-nm Chl form detectable in LHC II aggregates.

contributions from spectrally distant Chl forms via EET (with conservation of polarization) to a species spectrally close to λ_2. Further possibilities could be that the substructure arises because of excitonic splitting and/or vibronic contributions coupled to the electronic transition. The latter is not unlikely because 1) the Huang-Rhys factor (S) for LHC II was found to be of an appreciable magnitude ($S \geq 0.5$; cf. Reddy et al., 1994) as kindly remarked by one reviewer. Moreover, 2) cryptocyanine in solution provides an example for the vibronic origin of the NLPF spectral substructures (D. Leupold, B. Voigt, J. Ehlert, J. Hirsch, H. Stiel, K. Teuchner, and W. Sandner, unpublished results).

Varying λ_2 provides information on the connectivity between the Chl forms. Table 1 comprises these results. Probing, e.g., at $\lambda_2 = 645$ nm in LHC II trimers, subbands with maxima at 649, 660, and 669 nm contribute to the NLPF signal. Probing at 670 nm, the 660-, 669-, and 677-nm forms give contributions. Contributions from the 649-nm form are just as absent as those from the 684-nm form. In the same manner the results at $\lambda_2 = 685$ nm (third line in Table 1, left side) have to be interpreted.

Notably, the NLPF spectrum obtained when probing aggregated LHC II at $\lambda_2 = 670$ nm can be described by a single (sub-)band. This offers the possibility for a preliminary estimation of the extent of inhomogeneous broadening in the subband. Using the theoretical lineshape function for moderate inhomogeneous broadening (case 1) it follows that the experimental NLPF profile would be consistent with a model between the limits of pure homogeneous broadening and inhomogeneous broadening (maximally) up to Γ_{hom}. This is in agreement with the theoretical predictions of Jia et al. (1992). Moderate inhomogeneous broadening would result in an increase of the respective T_2 values by a factor of ~2. This approach provides the basis for the determination of the T_2 limits as given in Table 2.

The broad-range NLPF spectra obtained from aggregated LHC II differ significantly from their trimeric counterparts. Two main features emerge (Table 1, right side): 1) there is no unequivocal hint of a 669-nm subband; and 2) there are contributions from the 649-nm form in the NLPF signals

probed at 676 and 685 nm, and also, e.g., from the 677-nm form in the 645-nm signal. This might indicate that the depolarization of the excitation during EET in LHC II aggregates is less effective than within the trimeric form, but "uphill" EET is less probable for energetic reasons. A preliminary explanation may be that the subbands reflect at least in part excitonic splitting, thus rendering the number of subbands not necessarily identical with the number of "forms" (entities defined by their respective different environment). A final and unambiguous interpretation requires further experiments with a more dense distribution of NLPF probe wavelengths; this work is currently under way in our lab. Preliminary results with Chl *a* in diethyl-ether solution indicate only one species with dominating homogeneous behavior, very similar to Fig. 2 *a*.

Dephasing times

T_2 values were obtained from NLPF data with the probe wavelength closest to the respective subband according to Jennings et al. (1993) to avoid distortion, e.g., by EET. The T_2 values as displayed in Table 2 are (for each of the subbands) clearly in the sub-100-fs range. This holds true even for moderate inhomogeneous broadening (as indicated by the upper limits in Table 2). Thus, T_2 values obtained from NLPF experiments are consistent with the theoretical predictions of Kenkre and Knox (1976). Hence, the T_2 values derived here are considerably shorter than the ones (up to 4 ps) deduced by Bittner et al. (1991) from nonlinear absorption experiments with BBY particles (where LHC II is the dominating absorber, also). Remarkably, our T_2 for the 649-nm band (close to the 647-nm probe wavelength of Bittner et al. (1991) was the shortest observed. In our nonlinear absorption measurements (providing comparable excitation conditions) we have in no case observed similar nonlinear absorption phenomena as Bittner et al. (1991) did, neither in BBY particles nor in thylakoid suspensions (H. Lokstein, unpublished results).

As indicated in Table 2, the T_2 values for the subbands of the trimers show an increase from the short wavelength bands to the red-shifted ones, indicating that the Γ_{hom} values of the subbands are different. This is in conflict with the nearly constant FWHM in the model of Jennings et al. (1993), but consistent (especially for the broad FWHM of the band centered at 649 nm) with earlier nonlinear laser spectroscopic results (Leupold et al., 1989).

The present data suggest that there could even be some overlap with ultrafast EET as reported recently by Du et al. (1994), thus creating a very complex appearance of exciton dynamics in LHC II on the sub-ps time scale. Interesting in this respect are also the findings of a recent hole-burning study in LHC II (Reddy et al., 1994). The T_2-value of the red-most transition (at 680 nm) was found to be 10 ps at 4.2 K. The transition appeared to be largely inhomogeneously broadened. No long-wavelength forms (centered at 684 and 693 nm) have been detected at liquid helium temperature. The latter could be indicative, however, of a not yet understood structural alteration of the sample upon cooling. Other workers (Zucchelli et al., 1994) have reported the 684-nm band to be extremely temperature sensitive, vanishing at low temperature.

The seemingly contradictory broadening modes observed both at 4.2 K and RT can be largely reconciled with applying the model of Jia et al. (1992), predicting prevailing inhomogeneous broadening at 4 K (Γ_{inh} around 200 cm^{-1}, temperature-invariant) and homogeneous broadening becoming of paramount importance at RT.

To make our results directly comparable to the hole-burning data and to clarify the above apparent contradictions, an extension of the NLPF experiments to the low temperature region is in progress.

Pump-beam intensity dependence of the NLPF lineshapes

Further valuable information can be derived from the NLPF lineshapes when the pump intensity is varied. At the moment we defer discussion of the effects on the broad-range spectra, but examples of intensity dependence in the high-resolution NLPF spectra are given (Fig. 6). The T_1 values derived from such spectra at a certain λ_2 reflect the excited state lifetime(s) of the form(s) contributing to the respective signal (cf. Table 1). Note that $T_1 \geq 60$ ps cannot be resolved with the current apparatus. In principle one should be able to investigate the intensity dependence of the lifetimes in each subband, but this requires a more dense distribution of λ_2 and global analysis of the data. The NLPF profiles at $\lambda_2 = 670$ nm (Fig. 6) show considerable broadening with increasing pump intensity (which means shortening of the excited state lifetime). Most probably the lifetime shortening results from exciton-exciton annihilation, given that the

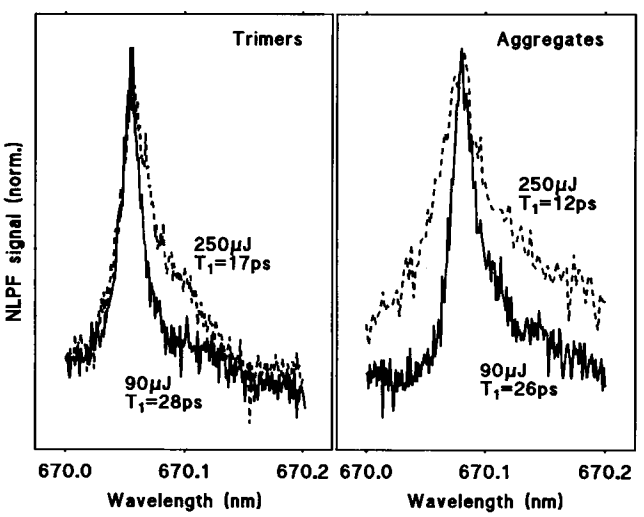

FIGURE 6 Excitation intensity dependence of the NLPF lineshapes (with high resolution around the resonance wavelength, $\lambda_1 = \lambda_2 = 670$ nm) in trimers and aggregates of LHC II.

effect exerted on LHC II-aggregates appears to be more pronounced than in the trimers. This is to be expected, since exciton annihilation has been shown to be critically dependent on the so-called domain size (array of pigments over which an exciton can "diffuse" during its lifetime), thus rendering aggregates with substantially larger domain sizes more susceptible for exciton annihilation (Geacintov and Breton, 1982; Nordlund and Knox, 1981). Both reported types of annihilation, singlet-singlet as well as singlet-triplet annihilation are to be expected for our experimental conditions (pulse duration of ~15 ns FWHM). Recently, on the basis of ultrafast absorbance transients under singlet-singlet annihilation conditions it was shown that the energy migration patterns in small and large aggregates of LHC II differ significantly from each other (V. Barzda, G. Garab, L. Gulbinas, and L. Valkunas, submitted for publication).

CONCLUSIONS

NLPF spectroscopy yields information otherwise not accessible for LHC II at physiological temperatures. NLPF 1) gives direct indication for spectral substructures (heterogeneity); 2) demonstrates differentiated energy transfer/coupling behavior between subbands in trimers and aggregates and thus, can probably help to reveal the "high-energy quenching" mechanism; 3) reveals the mode of absorption-band broadening of the Chl *a* and *b* Q_y bands; 4) yields ultrafast dephasing times of a few 10 fs under the assumption that dephasing in LHC II is a purely intra-Chl form process, which needs to be further investigated; and 5) indicates the occurrence of multiphoton processes (exciton-exciton annihilation).

This work was supported by the "Deutsche Forschungsgemeinschaft" (Le729/2–1). H. L. is indebted to the "Studienstiftung des deutschen Volkes" for support by a postgraduate fellowship.

REFERENCES

Allen, J. F. 1992. Protein phosphorylation in regulation of photosynthesis. *Biochim. Biophys. Acta.* 1098:275–335.

Arnon, D. I. 1949. Copper enzymes in chloroplasts. Polyphenol oxidase in *Beta vulgaris*. *Plant Physiol.* 24:1–15.

Barzda, V., L. Mustardy, and G. Garab. 1994. Size dependency of circular dichroism in macroaggregates of photosynthetic pigment-protein complexes. *Biochemistry.* 33:10837–10841.

Bassi, R., M. Silvestri, P. Dainese, I. Moya, and G. M. Giaccometti. 1991. Effects of a non-ionic detergent on the spectral properties and aggregation state of the light-harvesting chlorophyll a/b protein complex (LHCII). *J. Photochem. Photobiol. B Biol.* 9:335–354.

Bittner, T., J. Voigt, G. Kehrberg, H. J. Eckert, and G. Renger. 1991. Evidence for excited state absorption in PS II membrane fragments. *Photosynth. Res.* 28:131–139.

Brown, J. S. 1972. Forms of chlorophyll in vivo. *Annu. Rev. Plant Physiol.* 23:73–86.

Brown, J. S., and S. Schoch. 1981. Spectral analysis of chlorophyll-protein complexes from higher plant chloroplasts. *Biochim. Biophys. Acta.* 636: 201–209.

Du, M., X. Xie, L. Mets, and G. R. Fleming. 1994. Direct observation of ultrafast energy-transfer processes in light harvesting complex II. *J. Phys. Chem.* 98:4736–4741.

Eads, D. D., E. W. Castner, R. S. Alberte, L. Mets, and G. R. Fleming. 1989. Direct observation of energy transfer in a photosynthetic membrane: chlorophyll b to chlorophyll a transfer in LHC. *J. Phys. Chem.* 93:8271–8275.

Förster, T. 1948. Zwischenmolekulare Energiewanderung und Fluoreszenz. *Ann. Phys. (Leipzig).* 2:55–75.

Förster, T. 1965. Delocalized excitation and excitation transfer. *In* Modern Quantum Chemistry, Vol. III. O. Sinanoglu, editor. Academic Press, New York. 93–137.

French, C. S., J. S. Brown, and M. C. Lawrence. 1972. Four universal forms of chlorophyll a. *Plant Physiol.* 49:421–429.

Garab, G. 1993. Macrodomain organization of complexes in the thylakoid membrane. *In* Progress in Photosynthesis Research. Vol. 1. N. Murata, editor. Kluwer, Dordrecht. 171–178.

Garab, G., S. Wells, L. Finzi, and C. Bustamante. 1988. Helically organized macroaggregates of pigment-protein complexes in chloroplasts: evidence from circular intensity differential scattering. *Biochemistry.* 27:5839–5843.

Geacintov, N. E., and J. Breton. 1982. Exciton annihilation and other nonlinear high-intensity excitation effects. *In* Biological Events Probed by Ultrafast Laser Spectroscopy. A. A. Alfano, editor. Academic Press, New York. 157–191.

Hemelrijk, P. W., S. L. S. Kwa, R. van Grondelle, and J. P. Dekker. 1992. Spectroscopic properties of LHC-II, the main light-harvesting chlorophyll a/b protein complex from chloroplast membranes. *Biochim. Biophys. Acta.* 1098:159–166.

Horton, P., and A. V. Ruban. 1992. Regulation of photosystem II. *Photosynth. Res.* 34:375–385.

Ide, J. P., D. R. Klug, W. Kühlbrandt, L. B. Giorgi, and G. Porter. 1987. The state of detergent solubilized light-harvesting chlorophyll-a/b protein complex as monitored by picosecond time-resolved fluorescence and circular dichroism. *Biochim. Biophys. Acta.* 893:349–364.

Jansson, S. 1994. The light-harvesting chlorophyll a/b-binding proteins. *Biochim. Biophys. Acta.* 1184:1–19.

Jennings, R. C., R. Bassi, F. M. Garlaschi, P. Dainese, and G. Zucchelli. 1993. Distribution of the chlorophyll spectral forms in the chlorophyll-protein complexes of photosystem II antenna. *Biochemistry.* 32: 3203–3210.

Jia, Y., J. M. Jean, M. M. Werst, C. K. Chan, and G. R. Fleming. 1992. Simulations of the temperature dependence of energy transfer in the PSI core antenna. *Biophys. J.* 63:259–273.

Keller, D., and C. Bustamante. 1986. Theory of the interaction of light with large inhomogeneous molecular aggregates. II. Psi-type circular dichroism. *J. Chem. Phys.* 84:2972–2980.

Kenkre, V. M., and R. S. Knox. 1976. Optical spectra and excitation coherence. *J. Lumin.* 12/13:197–193.

Krawczyk, S., Z. Krupa, and W. Maksymiec. 1993. Stark spectra of chlorophylls and carotenoids in antenna pigment-proteins LHC-II and CP-II. *Biochim. Biophys. Acta.* 1143:273–281.

Krupa, Z., N. P. A. Huner, J. P. Williams, E. Maissan, and D. R. James. 1987. Development at cold-hardening temperatures. *Plant Physiol.* 84: 19–24.

Kühlbrandt, W., D. N. Wang, and Y. Fujiyoshi. 1994. Atomic model of plant light-harvesting complex by electron crystallography. *Nature.* 367: 614–621.

Kwa, S. L. S., H. van Amerongen, S. Lin, J. P. Dekker, R. van Grondelle, and W. S. Struve. 1992. Ultrafast energy transfer in LHC-II trimers from the Chl a/b light-harvesting antenna of Photosystem II. *Biochim. Biophys. Acta.* 1102:202–212.

Leupold, D., E. Neef, B. Voigt, F. Nowak, J. Ehlert, J. Hirsch, M. Bandilla, and H. Scheer. 1994. Substructure analysis of the bacterial antenna LH II by nonlinear polarization spectroscopy in the frequency domain. *Lithuanian J. Phys.* 34:339–343.

Leupold, D., H. Stiel, E. Klose, and P. Hoffmann. 1989. Search of "chlorophyll-forms" in vivo by non-linear laser spectroscopy. *Ber. Bunsenges. Phys. Chem.* 93:371–374.

Leupold, D., B. Voigt, J. Ehlert, H. Schroth, M. Bandilla, and H. Scheer. 1992. Ultrafast processes in bacterial antennas studied by nonlinear polarization spectroscopy (frequency domain). *In* Research in Photosynthesis, Vol. I. N. Murata, editor. Kluwer, Dordrecht. 109–111.

Leupold, D., B. Voigt, M. Pfeiffer, M. Bandilla, and H. Scheer. 1993. Nonlinear polarization spectroscopy (frequency domain) studies of excited state processes: the B800–850 antenna of *Rhodobacter sphaeroides*. *Photochem. Photobiol.* 57:24–28.

Lokstein, H., H. Härtel, P. Hoffmann, and G. Renger. 1993. Comparison of chlorophyll fluorescence quenching in leaves of wild-type with a chlorophyll-b-less mutant of barley (*Hordeum vulgare* L.). *J. Photochem. Photobiol. B Biol.* 19:217–225.

Lokstein, H., H. Härtel, P. Hoffmann, P. Woitke, and G. Renger. 1994. The role of light-harvesting complex II in excess excitation energy dissipation: an in-vivo fluorescence study on the origin of high-energy quenching. *J. Photochem. Photobiol. B Biol.* 26:175–184.

Mullineaux, C. W. 1993. Excitation-energy quenching in aggregates of LHC II chlorophyll-protein complex: a laser-induced optoacoustic study. *Biochim. Biophys. Acta.* 1143:235–238.

Mullineaux, C. W., A. A. Pascal, P. Horton, and A. R. Holzwarth. 1993. Excitation-energy quenching in aggregates of LHC II chlorophyll-protein complex: a time-resolved fluorescence study. *Biochim. Biophys. Acta.* 1141:23–28.

Nedbal, L., and V. Szöcs. 1986. How long does excitonic motion in the photosynthetic unit remain coherent? *J. Theor. Biol.* 120:411–418.

Neef, E., and S. Mory. 1991. Content of information of nonlinear polarization spectroscopy. *Exp. Techn. Physik.* 39:385–388.

Nibbering, E. T. J., D. A. Wiersma, and K. Duppen. 1991. Femtosecond Non-Markovian optical dynamics in solution. *Phys. Rev. Lett.* 66: 2464–2467.

Nordlund, T. M., and W. H. Knox. 1981. Lifetime of fluorescence from light-harvesting chlorophyll a/b proteins. Excitation intensity dependence. *Biophys. J.* 36:193–201.

Palsson, L. O., M. D. Spangfort, V. Gulbinas, and T. Gillbro. 1994. Ultrafast chlorophyll b-chlorophyll a excitation energy transfer in the isolated light harvesting complex, LHC II, of green plants. Implications for the organisation of chlorophylls. *FEBS Lett.* 339:134–138.

Reddy, N. R. S., H. van Amerongen, S. L. S. Kwa, R. van Grondelle, and G. J. Small. 1994. Low-energy exciton level structure and dynamics in light harvesting complex II trimers from the Chl a/b antenna complex of photosystem II. *J. Phys. Chem.* 98:4729–4735.

Saikan, S., and J. Sei. 1983. Experimental studies of polarization spectroscopy in dye solutions. *J. Phys. Chem.* 79:4146–4153.

Savikhin, S., H. van Amerongen, S. L. S. Kwa, R. van Grondelle, and W. S. Struve. 1994. Low-temperature energy transfer in LHC-II trimers from the Chl a/b light-harvesting antenna of Photosystem II. *Biophys. J.* 66:1597–1603.

Song, J. J., J. H. Lee, and M. D. Levenson. 1978. Picosecond relaxation measurements by polarization spectroscopy in condensed phases. *Phys. Rev. A.* 17:1439–1447.

van Grondelle, R. 1985. Excitation energy transfer, trapping and annihilation in photosynthetic systems. *Biochim. Biophys. Acta.* 811:147–195.

Zucchelli, G., P. Dainese, R. C. Jennings, J. Breton, F. M. Garlaschi, and R. Bassi. 1994. Gaussian decomposition of absorption and linear dichroism spectra of outer antenna complexes of photosystem II. *Biochemistry.* 33:8982–8990.